Damage Development in Bolt Bearing of Composite Laminates

Tseng-Hua Tsiang* and John F. Mandell†
Massachusetts Institute of Technology, Cambridge, Massachusetts

The buildup of damage in bolt-loaded specimens has been investigated. Destructive evaluation by staining, dissection, and microscopy was used to evaluate the complete three-dimensional geometry of the damage zone at several load levels and loading conditions for glass and graphite fiber-reinforced epoxy laminates with the stacking sequence $[[0/+45/-45]_3/0]_s$. The assumed stress hybrid finite element method was used to determine the elastic stress distributions, including simulations of no friction and no sliding. Three sets of tests are included: a fastened bolt joint in tension, a fastened bolt joint in compression, and a fastened bolt hole in tension. Complete damage characteristics and stress distributions are even ply by ply through the thickness as a function of load. The local strength around the hole boundary is examined pointwise by the Tsai-Hill criterion; the maximum stress criterion is then used to determine the failure mode. First-ply failure criteria are applied and compared with experiments. The three sets of tests indicate that the damage zones of the net-tension and bearing-compression regions are independent at both the initiation and failure stages. Implications for gross failure criteria are discussed, and the need for more sophisticated methods is demonstrated. Attempts have been made to correlate actual damage zones with Whitney-Nuismer distance parameters, but no physical interpretation of these parameters appears justified.

Introduction

THE fracture mechanisms of fiber composites are more complex than those of conventional isotropic materials. Initial damage in tensile zones often consists of splits that penetrate parallel to the fibers and through the thickness of each layer. The fracture process also generates debonding, delamination, and fiber breakage. Macromechanics alone cannot fully explain the behavior, but it can provide useful quantitative information for engineering design. Although micromechanics can take account of material inhomogeneity, its use in complicated boundary value problems is impractical. Earlier research[1-3] recommended a microscopic investigation accompanied by macroscopic analysis to better understand the fracture behavior of fiber composites.

Under increasing load, composites containing macroscopic discontinuities, such as notches, cutouts, and bolt connections, typically develop a zone of subcritical cracking around the discontinuity. This zone is called the damage zone and, in some respects, is analogous to a yield zone in homogeneous materials. The damage zone appears to be responsible for reducing the stress concentration factor and the sensitivity to the discontinuities. The development of the damage zone varies with such parameters as mechanical properties of fiber and matrix material, ply configuration, and stacking sequence, as well as loading conditions.[4-7] Damage zone extension and its effect on notch sensitivity have not been treated in sufficient detail by any theoretical model.

For laminates with unloaded holes, as well as for bolted joints, there apparently is localized matrix cracking around regions of peak stress, having an effect similar in some respects to reducing the composite to a bare fiber net, which has an averaging effect on the fiber stresses in the region of local damage. For correlating data for net-section tension failure in bolted joints, as well as for unloaded-hole data, an average stress criterion has been used effectively.[8-10] In this criterion, a characteristic distance away from the hole is assumed to be a material property independent of geometry, and the failure is assumed to occur when the average stress over this distance equals the unnotched laminate strength. However, the characteristic distance has not been quantitatively associated with actual damage dimensions in composites.

Two-dimensional models necessarily fail to consider the true three-dimensional character of the damage zone geometry. Advances in treatment of this problem, as well as confidence in using presently available methods, requires knowledge of the true nature of the damage zone for cases of interest. Very little information is available on the more complex bolted-connection case, where bearing as well as tensile damage zones may occur and interact. Many of the damage zone aspects appear to apply to bolted joints as well as to holes, with the additional effects of bolted-hole enlargement due to damage development.[9]

The present work characterizes the buildup of damage near bolted holes as a function of applied load. Destructive evaluation by staining, dissection, and microscropy is used to evaluate the complete three-dimensional geometry of the damage zone at several loading levels. For a better understanding of the relations between the damage progression and load-carrying ability, three sets of tests are studied (Fig. 1): 1) a bolted joint in tension, 2) bearing compression of a laminate containing a bolted joint, 3) simple tension of a laminate containing a bolted hole. Each case has been analyzed using the assumed stress finite element method.[11,12] Both the fiber/matrix interfacial bonding and interlaminar bonding are assumed to be perfect. The analyses presented are elastic solutions that do not model the observed damage; they are used to predict initial cracking and to better understand the qualitative aspects of the general problem.

Experimental Investigations

S-glass/epoxy and graphite/epoxy laminates, with the stacking sequence of $[[0/+45/-45]_3/0]_s$, are studied in the present work. The specimens are 1 in. wide with a ½-in.-diam hole. Table 1 indicates the corresponding mechanical properties of the laminates. A stainless-steel bolt

Presented as Paper 84-0916 at the AIAA/ASME/ASCE/AHS 25th Structures, Structural Dynamics and Materials Conference at Palm Springs, Calif., May 14-16, 1984; received June 18, 1984; revision received Sept. 21, 1984.

*Currently with Rohr Industries, Inc., Chula Vista, CA. Member AIAA.

†Principal Research Associate, Department of Materials Science and Engineering.

and steel washer are machined to achieve a close-fit joint. Clamping forces are applied by finger-tightening.

The experimental investigation of loaded holes comprised three sets of tests, which are illustrated in Fig. 2. In all cases, the 0° ply is oriented in parallel to the loading direction. Six specimens for each of the three sets of joint tests were loaded to failure. Due to the opacity of the material, some special techniques of damage observation are required. The technique employed in this work was to cut a specimen from the hole region, stain it with a colored or fluorescent dye, metallurgically wet-sand and polish or razor deply to the desired level through the thickness, and view in a microscope under polarized or ultraviolet light. The detailed geometry of the damage zone throughout the specimen thickness is characterized for each material after loading to various fractions of the failure load, to trace the development and expansion of the damage zone under increasing load. The load levels were selected in each set based upon the observation of progressive damage in the test specimens and breaks in the load-displacement curves, as shown in Fig 3. At least two specimens were tested at every load level in each set—a total of 170 specimens.

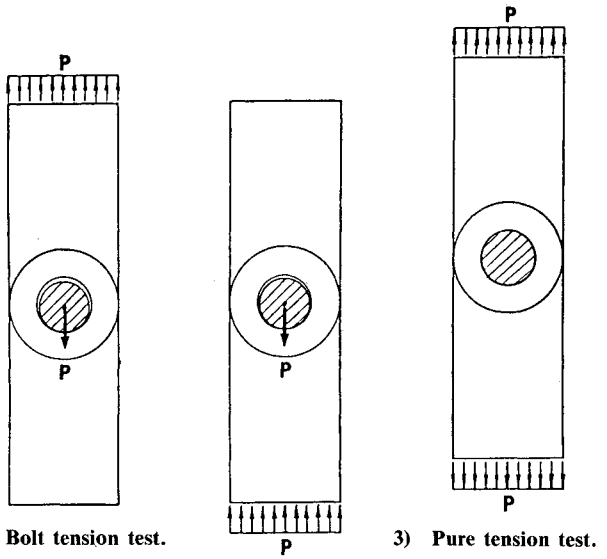

1) Bolt tension test. 2) Bearing compression test. 3) Pure tension test.

Fig. 1 Three sets of tests.

Characterization of Damage Development

Matrix cracks, fiber debonding, fiber breakage, interlaminar separation, and composite fractures were observed and recorded on laminar damage zone characterization diagrams, which contain a schematic sketch for each lamina or interply area, as illustrated in Figs. 4 and 5 for glass/epoxy and graphite/epoxy laminates, respectively. The complete characterization diagrams are available in Ref. 13. Typical microphotographs of the stained plies with damage are shown in Figs. 6 and 7 for glass/epoxy and graphite/epoxy laminates, respectively.

The size of the damage zone increases as the applied stress increases. The progression of such damage can be character-

Table 1 Mechanical properties of composite laminates[a]

Property	S-glass epoxy (S2/5208)	Graphite/epoxy (T3000/5208)
E_1, ksi	7000	19,000
E_2, ksi	2000	11,000
G_{12}, ksi	700	700
ν_{12}	0.25	0.25
T_1, ksi	200	175
T_2, ksi	7	7
C_1, ksi	125	150
C_2, ksi	30	20
S_{12}, ksi	11	11
E_X, ksi	2000	1380
E_Y, ksi	4000	8580
G_{XY}, ksi	1130	840
ν_{XY}	0.36	0.20
T_X, ksi	102	112

N.B.: $1,2$ = principal material axes, parallel and normal to fiber. X,Y = transverse and longitudinal axes of laminate. T,C,S = tensile, compressive, and shear strengths. E,G = Young's shear moduli. ν = Poisson's ratio.

[a] Ply properties were provided by Mr. D. Oplinger of AMMRC, Watertown, Mass.

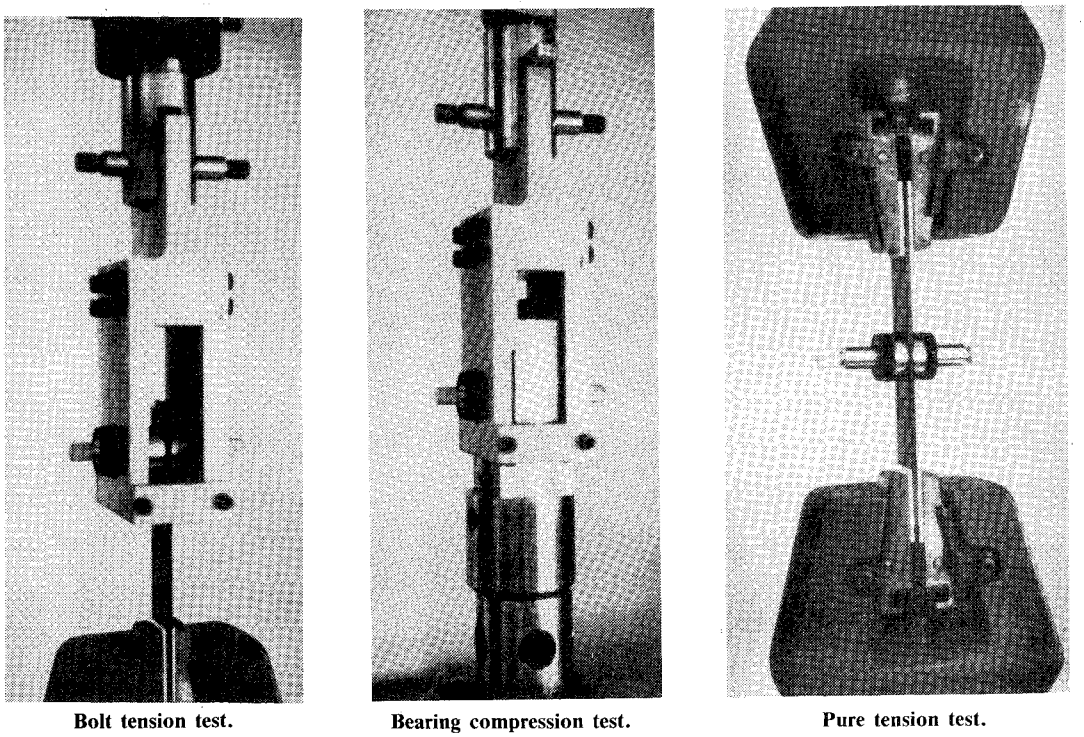

Bolt tension test. Bearing compression test. Pure tension test.

Fig. 2 Test setups.

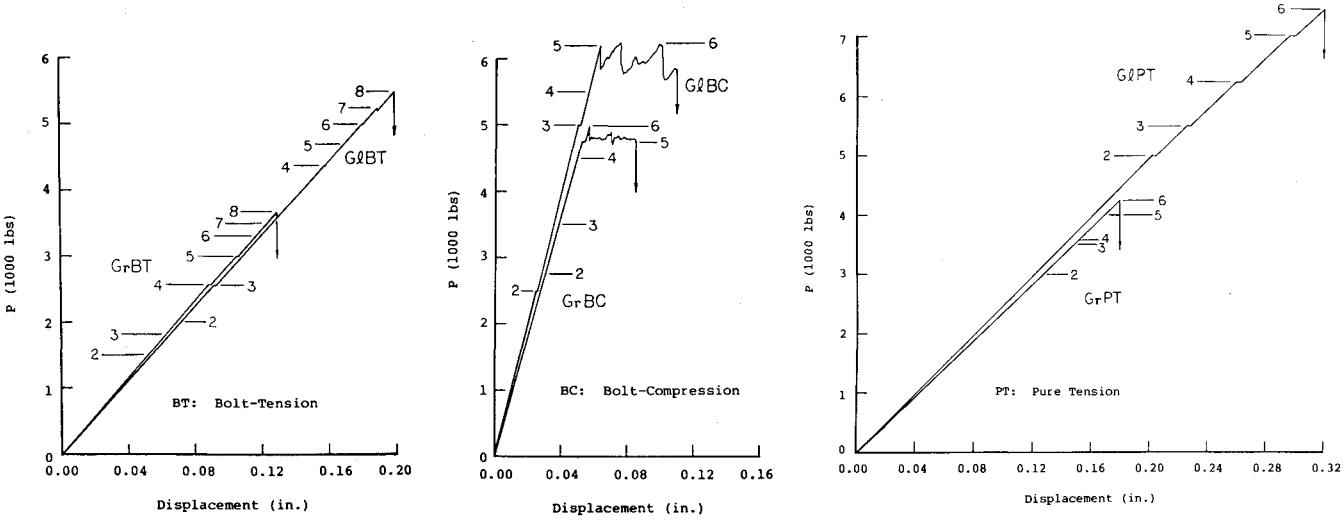

Fig. 3 Load-displacement curves of three test types.

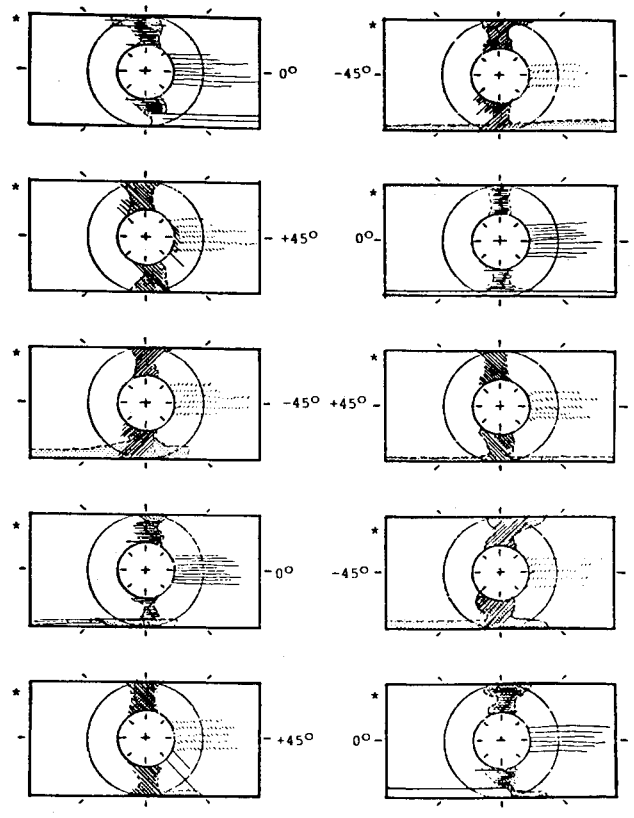

Fig. 4 Typical laminar damage zone characterization diagrams of S-glass/epoxy laminates (GℓBT-8 in Fig. 3).

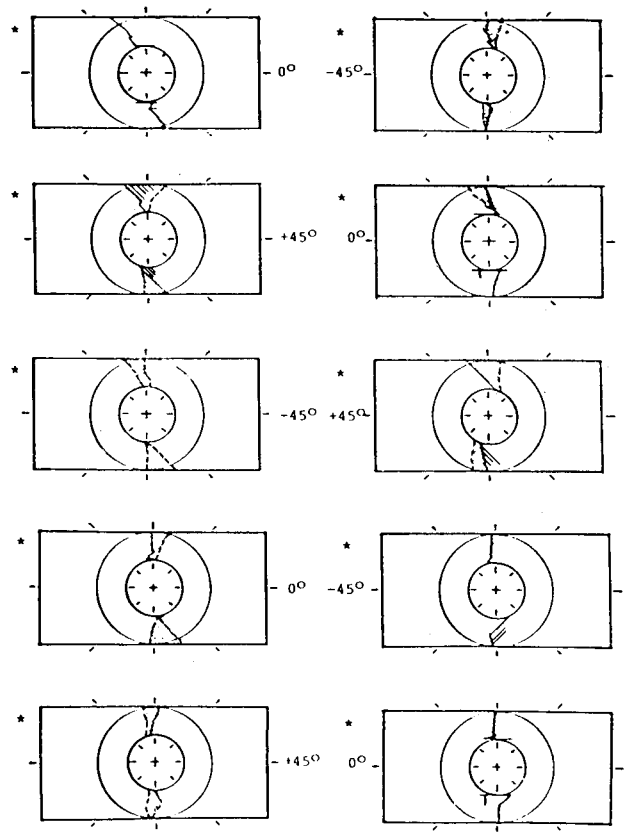

Fig. 5 Typical laminar damage zone characterization diagrams of graphite/epoxy laminates (GrBT-8 in Fig. 3).

ized by the dimensions of the zone at each load level. In the present study, the lengths of axial subcracks running along fibers at the neck (locations A and B) and bearing/contact (location C) locations in three categories of tests were measured. According to the failure mode, the lengths of the assorted subcracks were combined to obtain an average subcrack length $\bar{\ell}$. Figure 8 gives the average subcrack length in the 0° ply of both glass/epoxy and graphite/epoxy laminates as a stepwise function of the net-tension stress of the plate $\bar{\sigma}_N$. Due to the higher initial elastic stress concentration, the subcrack around the bolt-loaded hole initiates at lower stress than that around the plain hole under tension. A relatively long subcrack is observed for the glass/epoxy in comparison with that for the graphite/epoxy. Figure 9 gives the characteristic crack length in the bearing/contact region under bearing-compression and bolt-tension loads, respectively. In this failure mode, longer subcracks are also observed for the glass/epoxy laminate. For graphite/epoxy, there are no such subcracks developed under the bolt-tension load. Trans-fiber cracks are characterized for glass/epoxy laminates in both loaded and unloaded hole conditions, as shown in Fig. 10. As was the case with axial subcracks, trans-fiber cracks occur at lower stresses in bolt-loaded tension than in plain tension. Because of the complexity of fiber buckling and interply delamination, their development is indicated only on the laminar damage characterization diagrams.

Joint Failure Hypotheses

Prediction of first ply failure is of interest, and may be more practical than complete failure prediction in the absence of a full three-dimensional analysis including the damage zone. A popular failure criterion for a unidirectional fiber composite under a biaxial stress field is the Tsai-Hill criterion,[14] which is based on the distortional energy failure theory. This criterion can be expressed as

$$\frac{\sigma_L^2}{L^2}-\frac{\sigma_L\sigma_T}{L^2}+\frac{\sigma_T^2}{T^2}+\frac{\tau_{LT}^2}{S^2}=1$$

where L and T are either uniaxial tensile or compressive strengths in the L and T directions and S the ply in-plane shear strength of a unidirectional lamina with fibers in the L direction. In the present work, the local strength around the hole boundary is examined pointwise by the Tsai-Hill criterion, and then by using the maximum stress criterion to determine the failure mode.

The overall behavior of the laminate with a loaded or unloaded hole is first studied by using the two-dimensional orthotropic finite element model, as shown in Fig. 11. A cosine-distributed radial pressure is applied along the bottom half of the circumferential boundary of the hole in the plate. The axial boundary displacements on the far end of the plate are fixed. In-plane laminar stresses are then determined for each ply in a full-width plate by substituting multilayer elements into the equivalent displacement field, as determined in the two-dimensional analysis. The extreme frictional case is simulated by sticking the bolt to the hole boundary (zero sliding). This is accomplished in the finite element analysis by constraining all of the nodal displacements along the bottom semicircular boundary of the hole while a force is applied on the far end.

In the frictionless contact case, the transverse stress σ_x is in tension at the bearing/contact region and is much higher than the laminar transverse strength T at the experimental first-ply-failure load level. A very conservative prediction of first subcrack formation in this region is obtained. However, at the region of between 117 and 63 deg, the prediction of first subcrack formation is successful, as shown in Table 2a. A notable feature is that the shear stress τ_{xy} dominates the failure behavior at the $\theta=108$ deg location in the GℓBT loading condition, which is in agreement with the experimental observation. However, for the graphite/epoxy laminate, in the GrBT loading condition, it is too conservative. It is also seen that the prediction is conservative in the pure-tension loading condition for both glass/epoxy and graphite/epoxy laminates.

The no-slip contact analysis cannot predict the first ply failure at $\theta=90$ deg, because of the singularity associated with the edge of a stick-contact loading. However, at the bearing/contact region (θ between -11.25 and $+11.25$ deg), the stress distribution underneath the contact surface can be correlated to the subcrack failure mode. As shown in Table 2b, by applying the Tsai-Hill failure criterion to the 0° ply, the dominance of the transverse stress component σ_x is apparent. It is believed that the subcracks in the bearing/contact region are initiated at a position slightly beneath the contact surface, but no direct evidence of this has been found as cracks normally extend to the hole.

The point stress and average stress criteria predict failure when the stress at some characteristic distance ahead of the hole edge reaches the strength of the material, UTS.

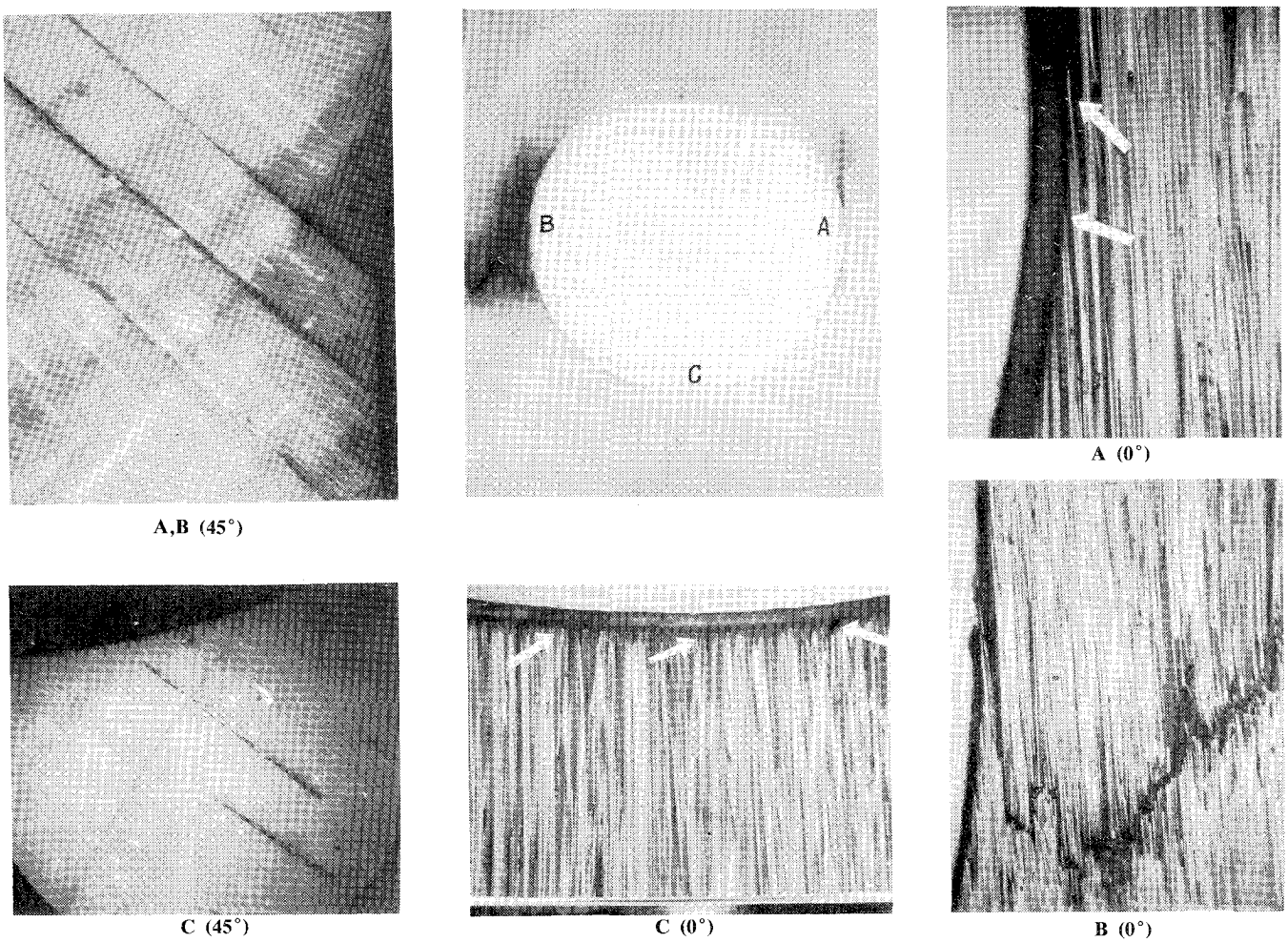

Fig. 6 Fracture modes of S-glass/epoxy laminates around the bolted hole.

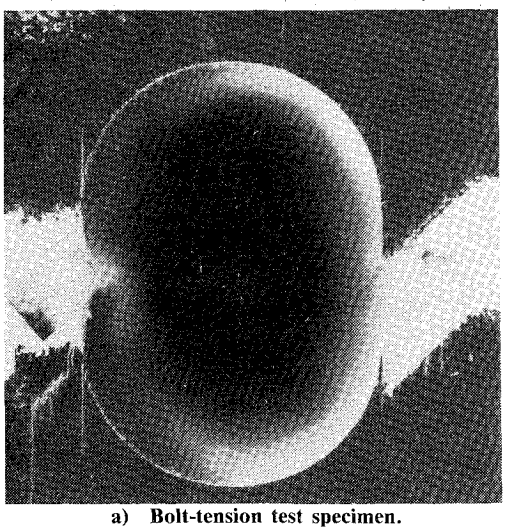

a) Bolt-tension test specimen.

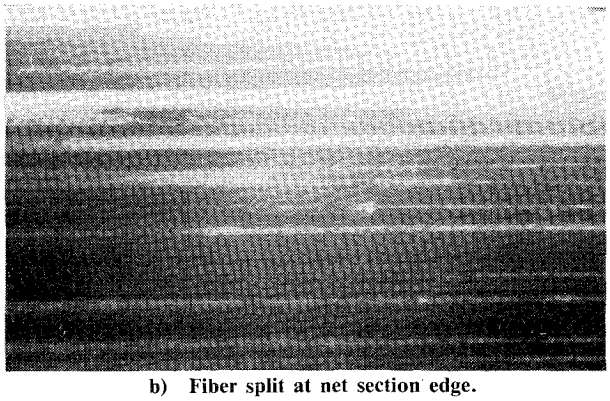

b) Fiber split at net section edge.

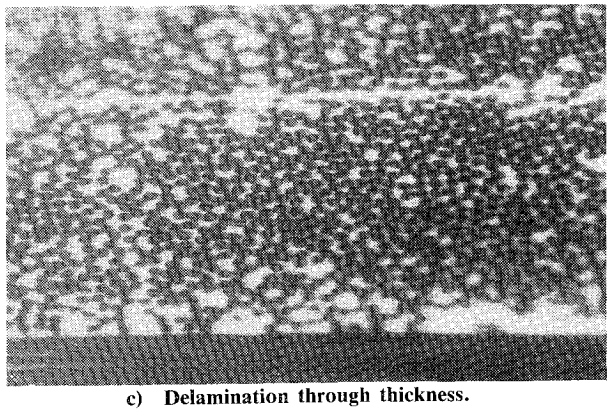

c) Delamination through thickness.

Fig. 7 Fracture modes of graphite/epoxy laminates around the bolted hole.

Table 2a First ply-failure prediction using the Tsai-Hill criterion at the experimental load

θ,[a] deg	$(\sigma_L/L)^2$	$(\sigma_T/T)^2$	$(\tau_{LT}/S)^2$	Tsai-Hill criterion	$(\sigma_L/L)^2$	$(\sigma_T/T)^2$	$(\tau_{LT}/S)^2$	Tsai-Hill criterion
		G/BT				G/PT		
117	0.12	0.22	0.61	0.95	0.27	0.07	1.06	1.40
108	0.26	0.11	0.71	1.08	0.67	0.07	1.51	2.25
99	0.44	0.00	0.36	0.80	1.25	0.01	0.88	2.14
90	0.56	0.09	0.03	0.65	1.80	0.05	0.06	1.86
81	0.54	0.10	0.06	0.71	1.72	0.05	0.40	2.13
72	0.37	0.18	0.49	1.04	1.28	0.00	1.55	2.83
63	0.18	0.19	1.07	1.42	0.71	0.22	2.01	2.95
		GrBT				GrPT		
117	0.26	0.21	0.60	1.07	0.27	0.02	0.35	0.65
108	0.80	0.34	0.81	1.93	1.00	0.22	0.67	1.54
99	1.72	0.17	0.53	2.42	2.47	0.17	0.45	3.09
90	2.56	0.02	0.10	2.68	4.10	0.01	0.02	4.13
81	2.51	0.07	0.02	2.60	4.46	0.00	0.26	4.72
72	1.47	0.21	0.44	2.12	3.14	0.02	1.00	4.11
63	0.51	0.30	1.19	2.00	1.40	0.21	1.27	2.87

N.B.: The value of $\sigma_L\sigma_T/L^2$ is much smaller than the other terms.

[a] θ is the angle between the point and loading directions; $\theta=0$ deg at the center of bearing/contact region; counterclockwise direction is positive.

Table 2b

$\bar{y}$,[b] in.	θ, deg	$(\sigma_L/L)^2$	$(\sigma_T/T)^2$	$(\tau_{LT}/S)^2$	Tsai-Hill criterion	$(\sigma_L/L)^2$	$(\sigma_T/T)^2$	$(\tau_{LT}/S)^2$	Tsai-Hill criterion
		G/BT				GrBT			
	11.25	0.92	0.01	0.07	1.08	1.24	0.00	0.07	1.31
0.00	0.00	1.02	0.04	0.00	1.01	1.20	0.02	0.00	1.20
	−11.25	0.93	0.01	0.12	1.03	1.33	0.00	0.03	1.33
0.036	0.00	0.96	0.82	0.01	1.74	1.38	0.15	0.00	1.50
0.071	0.00	1.06	4.90	0.06	5.89	1.64	0.69	0.01	2.27

[b] $\bar{y}$ = the distance below the bearing/contact surface.

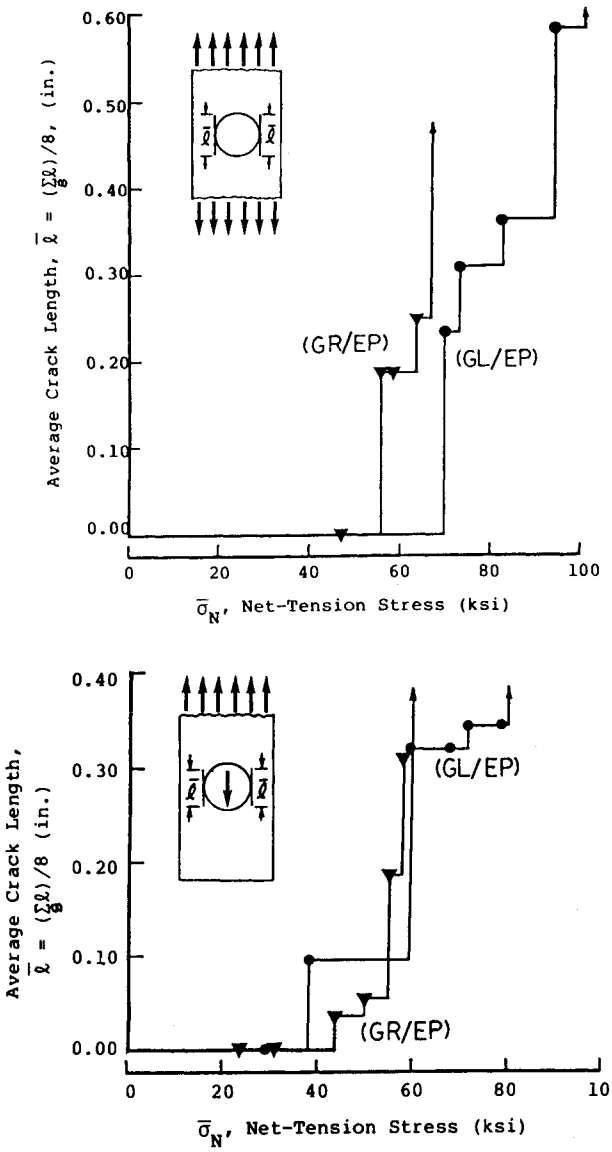

Fig. 8 Axial subcracks at the edges of hole (0° plies, under axial loading).

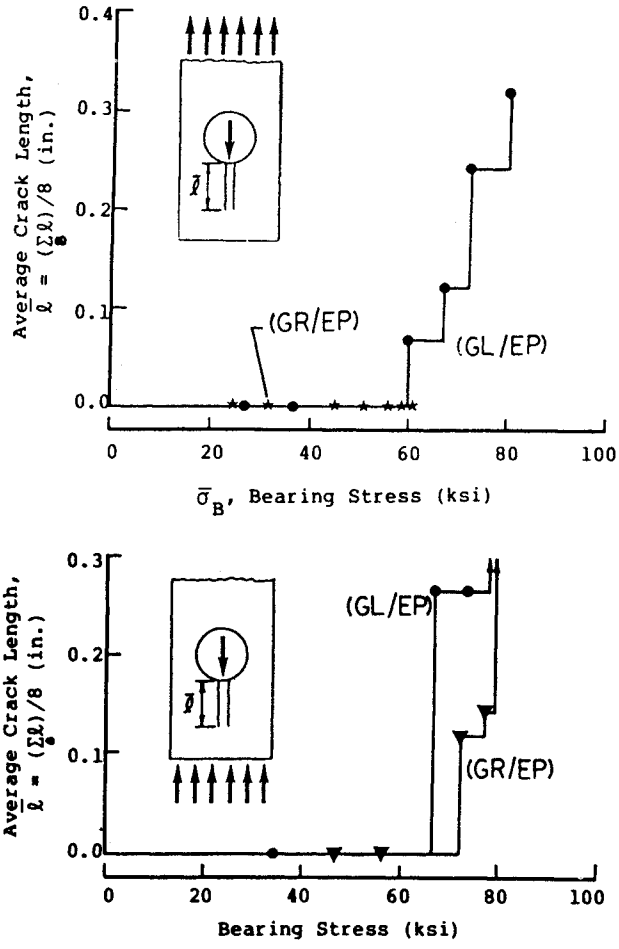

Fig. 9 0°-ply subcracks at the bearing/contact region (under axial loading).

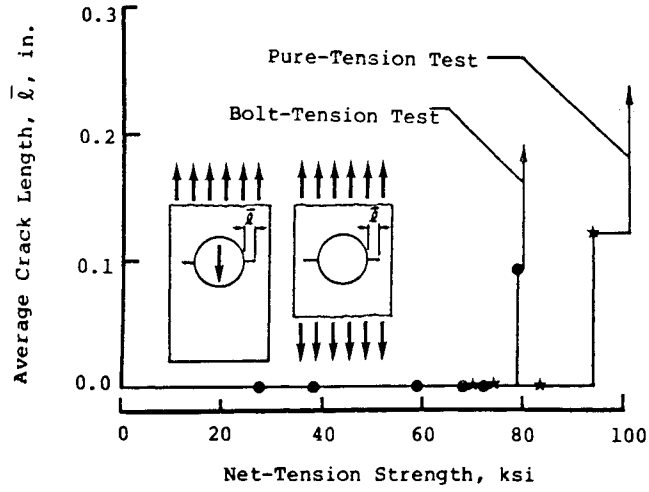

Fig. 10 Transfiber cracks in S-glass/epoxy laminates (0° plies).

However, evidence of damage shown in the experimental results do not support a direct physical interpretation of these parameters. Prior to the final stages of catastrophic failure, no damage in the range of the characteristic distance is observed across the net-tension section. In the 0° plies the damage even at loads approaching failure is simply a split in the fiber direction, with no dimension along the x axis. Damage in other plies and between plies is also inconsistent with the apparent values of the characteristic distance. Thus, the two-parameter failure models must be considered only as curve-fitting parameters that are useful in practice, but with no direct physical basis in the damage zone dimensions.

Discussion and Conclusions

As seen from the results obtained from the two extreme cases of no friction and no slip in the present analyses, a contact analysis with stick/slide conditions is necessary to obtain a precise stress distribution along the boundary of the hole[15,16]; however, such a computation would be costly. At the contacting edge, the solutions converge to finite values, which are equivalent to the contact stresses. With the additional friction-free edge conditions to the contact analysis, a more rapid convergence of the stresses is expected. However, the free-edge stress convergence study is in direct conflict with the notion of stress singularity in laminates, which is believed to be one of the factors responsible for delamination.[17-19] The analytical solutions of the stress singularity[20,21] have indicated that the region is so small that it corresponds to microscopic size which is not the concern of the macroscopic-scale analysis. Thus, there is currently a great deal of uncertainty regarding how to handle the delamination initiation problem in predicting failure. Based on available stress analyses, ply-stacking sequences may be chosen to decrease interlaminar stresses or to make the in-

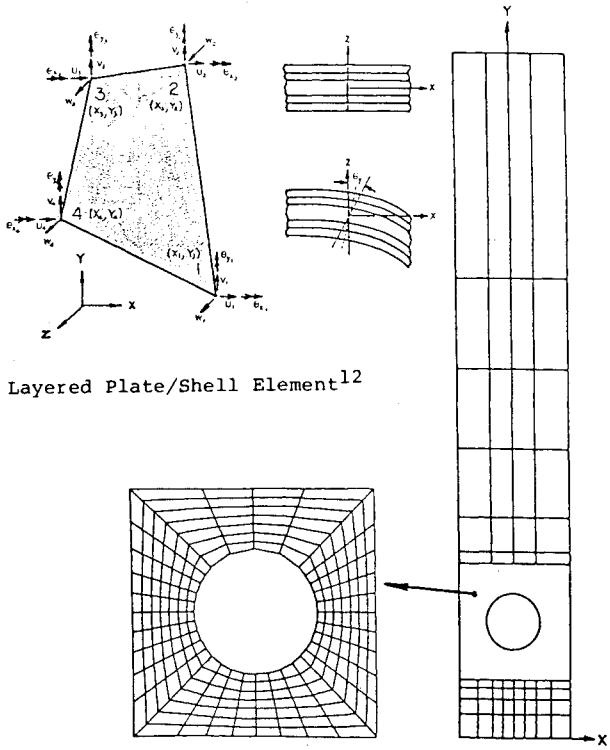

Fig. 11 Bolted joint finite element mesh.

terlaminar normal stress compressive. The delamination in the present study was observed only at loads well above where in-plane cracking occurred. The three sets of tests indicate that the damage zones of the net-tension and bearing-compression regions are independent at both the initiation and failure stages.

Because of the presence of friction at the intersurface between washer and plate, only the portion in the vicinity of the bolt head is in contact and beyond this area the washer is pulled away.[22-26] The generated clamp-up force can relieve the joint load transmitted by fastener shear. This may explain, in part, the high calculated stresses prior to cracking, and should be included in future analyses.

Due to the material anisotropy and local defects, the values of mechanical properties vary with different testing methods. Generally, the laminar tensile strength obtained from a four-point bending test is higher than that obtained from the uniaxial tensile coupon test, which has been adopted in the present study. Therefore, the first-ply-failure prediction can be in better agreement with our experimental results. This is supported by other studies of in-situ ply strength,[27] and may provide some explanation for the high stresses calculated at the load where the first damage is observed. A promising nondestructive test could be effective in detecting the initiation of subcritical cracking, and is recommended.

The overall ability to predict first-ply-failure, as shown in the present work, is not consistently good, apparently because of several factors as discussed previously. Gross failure prediction by the two-parameter models may work well in practice, but obviously the distance parameters do not correspond simply with the physical damage observed. Therefore, this is still a problem that is not very well handled with current technology.

Acknowledgment

This work was supported by the Army Materials and Mechanics Research Center through Contract DAAG-46-81-C-0010.

References

[1]Mandell, J. F., Wang, S. S., and McGarry, F. J., "Fracture of Graphite Fiber Reinforced Composites," AFML-TR-73-142, July 1973.

[2]McGarry, F. J., Mandell, J. F., and Wang, S. S., "Fracture of Fiber Reinforced Composites," *Polymer Engineering and Science*, Vol. 16, Sept. 1976, pp. 609-614.

[3]Lin, K. Y., "Fracture of Filamentary Composite Materials," Ph.D. Thesis, Dept. of Aeronautics and Astronautics, Massachusetts Institute of Technology,, Cambridge, Mass., Feb. 1977.

[4]Mandell, J. F., McGarry, F. J., Im, J., and Meier, U., "Fiber Orientation, Crack Velocity and Cyclic Loading Effects on the Modes of Crack Extension in Fiber Reinforced Plastics," *Failure Modes in Composites II*, edited by Fleck and Mehan, 1974, pp. 33-67.

[5]Mandell, J. F., Wang, S. S., and McGarry, F. J., "The Extension of Crack Tip Damage Zones in Fiber Reinforced Plastic Laminates," *Journal of Composite Materials*, Vol. 9, July 1975, pp. 266-287.

[6]Steiner, P. W., "Damage Zone in Notched Graphite/Epoxy Plate," M.S. Thesis, Ocean Engineering Dept., Massachusetts Institute of Technology, Cambridge, Mass., Sept. 1980.

[7]Freeman, S. M., "Damage Progression in Graphite-Epoxy by a Deplying Technique," AFWAL-TR-81-3157, Dec. 1981.

[8]Whitney, J. M. and Nuismer, R. J., "Stress Fracture Criteria for Laminated Composites Containing Stress Concentrations," *Journal of Composite Materials*, Vol. 8, July 1974, pp. 253-265.

[9]Oplinger, D. W., "On the Structural Behaviour of Mechanically Fastened Joints in Composite Materials," *Proceedings of the 4th Conference of Fiber Composites in Structural Design*, San Diego, Calif., 1978, pp. 575-602.

[10]Daniel, I. M., "Behaviour of Graphite/Epoxy Plates with Holes under Bi-Axial Loading," *Experimental Mechanics*, Jan. 1980, pp. 1-8.

[11]Pian, T. H. H., "Derivation of Element Stiffness Matrices by Assumed Stress Distributions," *AIAA Journal*, Vol. 2, 1964, pp. 1333-1336.

[12]Spilker, R. L., Chou, S. C., and Orringer, O., "Alternative Hybrid-Stress Elements for Analysis of Multilayer Composite Plates," *Journal of Composite Materials*, Vol. 11, 1977, pp. 51-70.

[13]Tsiang, T-H., "Damage Development in Fiber Composites Due to Bearing," Sc.D. Thesis, Dept. of Materials Science and Engineering, Massachusetts Institute of Technology, Cambridge, Mass., Feb. 1983.

[14]Tsai, S. W., "Strength Theories of Filamentary Structures," *Fundamental Aspects of Fiber Reinforced Plastic Composites*, edited by R. T. Schwartz and H. S. Schwartz, Interscience, New York, 1968, Chap. 1.

[15]Oplinger, D. W., "Stress Analysis of Composite Joints," *Advances in Joining Technology*, edited by J. J. Burke and A. E. Gorum, 1976, pp. 405-452.

[16]Ojalvo, I., "Survey of Mechanically Fastened Splice-Joint Analysis," *Advances in Joining Technology*, edited by J. J. Burke and A. E. Gorum, 1976, pp. 379-403.

[17]Wang, S. S. and Choi, I., "Boundary-Layer Effects in Composite Laminates: Part I: Free-Edge Stress Singularities; Part 2: Free-Edge Stress Solutions and Basic Characteristics," *Journal of Applied Mechanics*, Vol. 49, 1982, pp. 541-560.

[18]Zwier, R. I., Ting, T. C. T., and Spilker, R. L., "On the Logarithmic Singularity of Free-Edge Stress in Laminated Composites Under Uniform Extension," *Journal of Applied Mechanics*, Vol. 49, 1982, pp. 561-569.

[19]Zwier, R. I. and Ting, T. C. T., "Singularity of Contact-Edge Stress in Laminated Composites Under Uniform Extension," *Journal of Composite Materials*, Vol. 17, Jan. 1982, pp. 49-62.

[20]Ting, T. C. T. and Chou, S. C., "On the Nature of Stress Singularities in Anisotropic Layered Composites," *Advances in Aerospace Structures and Materials*, AD-03, ASME, Winter Annual Meeting, 1982, pp. 65-69.

[21]Chou, S. C., "Delamination of T300/5208 Graphite/Epoxy Laminates," *Proceedings of the Second USA-USSR Symposium on Fracture of Composite Materials*, edited by G. Sih and V. Tawuzs, Noordhoff, the Netherlands, 1981, pp. 231-248.

[22]Cullimore, M. S. G. and Upton, K. A., "The Distribution of Pressure Between Two Flat Plates Bolted Together," *International Journal of Mechanical Science*, Vol. 6, 1964, pp. 13-25.

[23]Stockdale, J. H. and Matthews, F. L., "The Effect of Clamping Pressure of Bolt Bearing Loads in Glass Fiber-Reinforced Plastics," *Composites*, Vol. 7, Jan. 1971, pp. 34-38.

[24]Gould, H. H. and Mikic, B. B., "Areas of Contact and Pressure Distribution in Bolted Joints," *Journal of Engineering for Industry*, Vol. 94, 1972, pp. 864-870.

[25]Cullimore, M. S. G. and Eckhart, J. B., "Distribution of the Clamping Pressure in Friction-Grip Bolted Joints," *Structural Engineering*, Vol. 52, 1974, pp. 129-131.

[26]Collings, T. A., "The Strength of Bolted Joints in Multi-Directional CFRP Laminates," *Composites*, Vol. 8, Jan. 1977, pp. 43-55.

[27]Flaggs, D. L. and Kural, M. H., "Experimental Determination of the In-Situ Transverse Lamina Strength in Graphite/Epoxy Laminates," *Journal of Composite Materials*, Vol. 16, March 1982, pp. 103-116.